analytical chemistry

Article

pubs.acs.org/ac

Near Infrared Fluorescent Trypsin Stabilized Gold Nanoclusters as Surface Plasmon Enhanced Energy Transfer Biosensor and in Vivo Cancer Imaging Bioprobe

Jing-Min Liu,[†] Jia-Tong Chen,[‡] and Xiu-Ping Yan*[,†]

[†]State Key Laboratory of Medicinal Chemical Biology, and Research Center for Analytical Sciences, College of Chemistry, Nankai University, 94 Weijin Road, Tianjin 300071, China

[‡]Department of Biochemistry and Molecular Biology, College of Life Sciences, Nankai University, 94 Weijin Road, Tianjin 300071, China

Supporting Information

ABSTRACT: The simplicity of the green-synthesized routine and the availability of surface modification of diverse bioactive molecules make noble metal nanostructures highly suitable as multifunctional biomaterials for biological and biomedical application. Here, we report the preparation of trypsin stabilized gold nanoclusters (try-AuNCs) with near-infrared fluorescence for biosensing heparin based on surface plasmon enhanced energy transfer (SPEET) and folic acid (FA) modified try-AuNCs for in vivo cancer bioimaging. The SPEET/try-AuNCs fluorescence biosensor was designed via heparin mediated energy transfer between try-AuNCs and cysteamine modified gold nanoparticles (cyst-AuNPs). The developed SPEET/try-AuNCs fluorescence biosensor allowed sensitive and selective detection of heparin with a linear range of 0.1−4.0 μg mL^{-1} and a detection limit (3s) of 0.05 μg mL^{-1}. The relative standard deviation for eleven replicate detections of 2.5 μg mL^{-1} heparin was 1.1%, and the recoveries of the spiked heparin in human serum samples ranged from 97% to 100%. In addition, folic acid was immobilized on the surface of try-AuNCs to ameliorate the specific affinity of AuNCs for tumors, and the near-infrared fluorescent FA-try-AuNCs were applied for in vivo cancer imaging of high folate receptor (FR) expressing Hela tumor. In vivo study of the dynamic behavior and targeting ability of FA-try-AuNCs probe to Hela tumor bearing mice and normal nude mice validated the high specific affinity of FA-try-AuNCs probe to FR positive tumors. The results show that the prepared try-AuNCs have great potential as multifunctional biomaterials for biosensing biomolecules with SPEET mode and in vivo cancer imaging with high targeting ability.

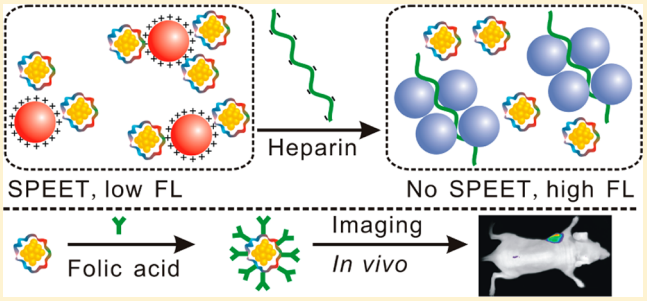

Molecular biosensing and bioimaging, the biotechnology of the ability to probe the life reaction within the living human body and understand its biological complexities for the treatment of disease, has contributed a lot in the development of biomedical and biological science.[1−3] The key step is to design sensing and imaging agents that make molecular processes quantitative, visible, quantifiable, and traceable over time, aiming to realize the noninvasive study of biological processes in vivo at the cellular and molecular level.[4−8] The feasible method and advanced biomaterials with multifunction and excellent biocompatibility are thus highly demanded. Fluorescent bioimaging with high sensitivity, multiplex detection capabilities, activatable property, and low equipment cost has attracted the most attention. Conventional fluorophores for fluorescent bioimaging including organic dyes and engineered fluorescent proteins suffer from poor photostability, while the considered promising alternative, semiconductor quantum dots (QDs), still have some limitations, such as large particle size upon functionalization, tendency to aggregate, and potential toxicity, which hinder further application in bioimaging.[9]

Noble metal nanoclusters (NMNCs), a new type of luminescent nanomaterials, have recently attracted great interest.[9,10] NMNCs are composed of a few to a hundred atoms, with sizes approaching to the Fermi wavelength of electrons, and exhibit molecule-like properties including discrete electronic states and size-dependent fluorescence.[11] Owing to their strong photoluminescence, ultrasmall size, excellent biocompatibility and photostability, and the availability of multifunctional groups for covalent linkage of diverse bioactive molecules, NMNCs have emerged as powerful and multifunctional biomaterials for molecular biosensing[12−22] and bioimaging.[11,23−30]

Noble metal nanoparticles (NMNPs) possess strong light scattering and absorption ability, known as surface plasmon resonance (SPR), which arises from the resonant oscillation of their free electrons in the presence of light with particular

Received: December 12, 2012
Accepted: February 18, 2013
Published: February 18, 2013

frequency.[31−34] Due to its large surface-to-volume ratio, nanometal surface follows the expression given by the surface energy transfer (SET) instead of the usual dipole−dipole type of Förster resonance energy transfer (FRET).[35] SET allows a 22 nm detection length scale against 10 nm detection length in FRET, which obviates the restriction of less signal alternation in biosensing.[36,37] It was reported that the unique SPR property of NMNPs produces a highly sensitive photoluminescence quenching behavior via a surface plasmon enhanced energy transfer (SPEET) mechanism between NMNPs and NMNCs, and such a new energy transfer mode possesses great potential for biomedical and biological applications.[38]

Here, we report the preparation of trypsin stabilized gold nanoclusters (try-AuNCs) with near-infrared (NIR) fluorescence and their application in designing a SPEET biosensor for heparin and bioprobe for in vivo cancer imaging. Heparin is a naturally occurring sulfated polysaccharide, highly negatively charged, formed predominantly by a repeating unit of trisulfated disaccharide, and widely used as the anticoagulant during numerous surgical procedures involving extracorporeal blood circulation.[39−42] Monitoring of heparin levels is of crucial significance to avoid the risk such as hemorrhage and thrombocytopenia during the surgery and the anticoagulant therapy, because overdose of heparin often causes a potentially fatal bleeding complication.[43] Various techniques and methods have been established for the determination of heparin, including fluorescent,[44−46] colorimetric,[43,47,48] and electrochemical methods.[49,50] In the present work, sensitive and selective detection of heparin was realized on the basis of the SPEET between try-AuNCs and cysteamine modified gold nanoparticles (cyst-AuNPs). Moreover, try-AuNCs were successfully used to target tumor (Hela) via folic acid (FA) surface modification for in vivo bioimaging, and the FA-try-AuNCs fluorescence probe gave high selective affinity for folate receptor (FR) positive Hela tumor. These two major application assays proved that our prepared try-AuNCs are multifunctional and feasible biomaterials with great potential for further biological and biomedical investigation.

EXPERIMENTAL SECTION

Chemicals and Materials. All reagents were of the highest available purity and at least of analytical grade. Ultrapure water (Wahaha, Hangzhou, China) was used throughout all experiments. Heparin and cysteamine were purchased from Aladdin (Shanghai, China). Chloroauric acid ($HAuCl_4{\cdot}4H_2O$) was purchased from Sinopharm Chemical Reagent Co. Ltd. (Shanghai, China). Trypsin, folic acid, human serum albumin (HSA), lysozyme, cytochrome C (cyt-C), immunoglobulin (IgG), insulin, thrombin, transferrin, fibrinogen, hemoglobin, myoglobin, zonolysin, glucose, lactic acid, glutathione (GSH), cysteine, and other amino acids were purchased from Sigma (St. Louis, MO, USA). H_3PO_4, HAc, H_3BO_3, NaOH, $NaH_2PO_4{\cdot}2H_2O$, $Na_2HPO_4{\cdot}12H_2O$, $NaBH_4$, and $Na_2B_4O_7{\cdot}10H_2O$ were all obtained from Guangfu Fine Chemical Research Institute (Tianjin, China). Britton-Robinson (BR) buffer solution (10 mM H_3PO_4−10 mM HAc−10 mM H_3BO_3) and phosphate buffer solution (PBS) (136.9 mM NaCl, 2.68 mM KCl, 8.1 mM Na_2HPO_4, 1.47 mM KH_2PO_4, pH 7.4) were used as the biosensing assay buffer and bioimaging assay buffer, respectively. All the glassware was cleaned with aqua regia (HCl/HNO_3 = 3:1, v/v) and thoroughly rinsed with ultrapure water before use.

Instrumentation. All fluorescence measurements were performed on a Hitachi F-4500 fluorescence spectrophotometer equipped with a plotter unit and a quartz cell (1 cm × 1 cm). All data were collected under the following conditions: photomultiplier tube (PMT) voltage, 700 V; excitation and emission slits, 10 nm; excitation wavelength, 520 nm. The absorption spectra were recorded on a UV-3600 UV−vis-NIR spectrophotometer (Shimadzu, Japan) with 1 cm path-length cells. In vivo fluorescence images of the mice were obtained with a NightOWL LB 983 in vivo Imaging System (Berthold, Bad Wildbad, Germany). The excitation filter was set as 530 nm, and the emission filter was set as 700 nm. Fluorescence images were recorded by the CCD camera with constant exposure time. In vitro cytotoxicity of the probe was assessed using the cell counting assay, and cell numbers were counted with a Coulter Particle Size Analyzer (Beckman Coulter, High Wycombe, UK). X-ray photoelectron spectroscopy (XPS) measurements were carried out on a Axis Ultra DLD spectrometer fitted with a monochromated Al Kα X-ray source (hν = 1486.6 eV), hybrid (magnetic/electrostatic) optics, and a multichannel plate and delay line detector (Kratos Analytical, Manchester, UK). Six spectra in the desired binding energy range were averaged. The samples were spotted as drop cast films on the sample stub and dried. The energy resolution of the spectrometer was set at 0.1 eV at a pass energy of 20 eV for typical measurements. Fourier transform infrared (FT-IR) spectra (4000−400 cm^{-1}) in KBr were recorded on a Magna-560 spectrometer (Nicolet, Madison, WI). Matrix assisted laser desorption ionization time of flight mass spectrometry (MALDI-TOF-MS) analysis was performed on an Autoflex III MALDI-TOF mass spectrometer (Bruker, Bremen, Germany) equipped with a 337-nm nitrogen laser, an ion source, delayed-extraction electronics, a high-resolution timed ion selector, and a 2-GHz digitizer. Before MALDI-TOF-MS analysis, the try-AuNCs were purified by centrifugal filtration twice at 6000 rpm for 30 min through Amicon Ultra-15 Centrifugal Filter Unit with Ultracel-50 membrane with a cutoff of 30 kDa (Millipore, Billerica, MA, USA) and resuspended in ultrapure water. Then, 1 mL of try-AuNCs solution (5 μM) or trypsin solution (5 μM) was typically mixed with equal volume of premade sinapinic acid matrix solution (prepared in a 1:3 mixture of acetonitrile and 0.1% trifluoroacetic acid), deposited onto the MTP 384 stainless steel target, and allowed to dry at room temperature. Circular dichroism (CD) assays were measured on a Jasco J-715 spectropolarimeter at ambient temperature (cell length: 1 cm; data pitch: 0.1 nm; bandwidth: 1 nm; scanning speed: 500 nm min^{-1}; accumulation: 3). The Raman measurement was performed on a RFS100/S FT-RAMAN spectrometer (Bruker, Germany) with 1064 nm laser excitation. The try-AuNCs solution (40 mM) was frozen to solid powder by a LGJ-22 vacuum freeze-dryer (SaiBo, Hefei, China) for the XPS, FT-IR, and Raman analyses.

The morphology and microstructure of the prepared nanostructures were characterized by high resolution transmission electron microscopy (HRTEM) on a JEM-2100F field emission transmission electron microscope (JEOL, Japan) operating at a 200 kV accelerating voltage. The samples for HRTEM were obtained by drying sample droplets on a 230-mesh Cu grid coated with a lacey carbon film. The decay curves of try-AuNCs fluorescence emission at 690 nm excited by the solution of BBQ pumped by a N_2 laser at 380 nm were recorded on a PTI QM/TM/NIR system (Birmingham, NJ, USA), and the lifetime was calculated using the Felix 32

dx.doi.org/10.1021/ac303603f | Anal. Chem. 2013, 85, 3238−3245

advanced fluorescence software. The fluorescence quantum yield (QY) of try-AuNCs was determined on an FLS920 spectrometer with an integration sphere attachment under excitation of 380 nm (Edinburgh, UK). The concentration of try-AuNCs was determined by element analysis (^{197}Au) with inductively coupled plasma mass spectrometry (ICPMS, Thermo Elemental X7). The try-AuNCs were thoroughly digested by aqua regia and diluted with 2% HNO_3 before ICPMS analysis. Determination of the zeta potential (ζ) of heparin, try-AuNCs, cyst-AuNPs, and the serum proteins in BR buffer (10 mM, pH 5.0) was performed on a Malvern Zetasizer 3000HSa (He−Ne laser, λ = 632.8 nm).

Synthesis of Try-AuNCs. The try-AuNCs were synthesized by a previously one-pot green method with some modifications.[51] Briefly, 10 mL of $HAuCl_4$ solution (10 mM, 37 °C) was added to 10 mL of trypsin solution (30 mg mL^{-1}, 37 °C) under vigorous stirring. After a 10 min incubation, NaOH solution (1 M) was introduced to adjust the reaction media pH to 12, and the reaction was allowed to proceed under vigorous stirring in the dark at 37 °C for 36 h. The as-synthesized try-AuNCs were purified by centrifugal filtration at 6000 rpm for 30 min through an Amicon Ultra-15 Centrifugal Filter Unit with Ultracel-50 membrane with a cutoff of 30 kDa (Millipore, Billerica, MA, USA), and the try-AuNCs were resuspended in ultrapure water. The purified try-AuNCs were stored at 4 °C in the dark, and the fluorescence was stable for at least 6 months.

Bioconjugation of Try-AuNCs with Folic Acid. Try-AuNCs were conjugated with folic acid using a zero-length cross-linker 1-ethyl-3-[3-dimethylaminopropyl] carbodiimide hydrochloride (EDC) according to the reported method.[52] FA was activated to become amine-reactive by linking with EDC. Typically, 25 mg of EDC was mixed with 10 mg of FA in 500 μL of PBS (136.9 mM NaCl, 2.68 mM KCl, 8.1 mM Na_2HPO_4, 1.47 mM KH_2PO_4, pH 7.4). After 5 min of incubation at room temperature with probe sonication, the mixture was added to 300 nmol of try-AuNCs dissolved in 3 mL of PBS, and the reaction proceeded for 2 h at room temperature in dark under continuous stirring. The obtained crude products were then purified by centrifugal filtration at 6000 rpm for 30 min through the Amicon Ultra-15 Centrifugal Filter Unit with Ultracel-50 membrane with a cutoff of 30 kDa to remove the excessive folic acid, and the FA-try-AuNCs were resuspended in PBS.

Synthesis of Cyst-AuNPs. The cysteamine stabilized AuNPs were prepared according to a published protocol.[41] Briefly, 400 μL of cysteamine solution (213 mM) and 2.23 mL of $HAuCl_4$ solution (25.4 mM) were mixed with 37.5 mL of H_2O. After stirring for 20 min at room temperature, 10 μL of $NaBH_4$ solution (10 mM) was added, and the mixture was vigorously stirred for 30 min at room temperature in the dark. The obtained win-red solution was stored at 4 °C in the dark for further use.

Procedures for Developing SPEET Biosensor. To investigate the quenching mechanism of cyst-AuNPs for try-AuNCs, 50 μL of try-AuNCs solution (20 mM) was mixed with 500 μL of BR buffer (40 mM, pH 5.0) and diluted to 2 mL by ultrapure water. Then, 20 μL of cyst-AuNPs solutions with various concentrations were added, and the fluorescence was measured immediately. The final concentrations of cyst-AuNPs were in the range of 0.02−2 nM.

To evaluate the kinetics of the interaction between heparin-cyst-AuNPs and try-AuNCs, 300 μL of cyst-AuNPs solution (2 nM), 1200 μL of ultrapure water, and 500 μL of BR buffer (40 mM, pH 5.0) were sequentially added to the test tube. Twenty μL of heparin standard solution with three different concentrations was then added, and the mixture was incubated for 20 min. After 50 μL of try-AuNCs solution (20 mM) was added to the mixture, the fluorescence emission spectra of try-AuNCs were recorded with an interval of 10 s.

To evaluate the kinetics of the interaction between cyst-AuNPs and heparin, 300 μL of cyst-AuNPs solution (2 nM) was mixed with 500 μL of BR buffer (40 mM, pH 5.0) and diluted to 2 mL with ultrapure water. Twenty microliters of heparin solutions with three different concentrations was added, and the absorption spectra were recorded with an interval of 1 min.

To examine the pH effect on the interaction between cyst-AuNPs and heparin, 300 μL of cyst-AuNPs solution (2 nM) was mixed with 500 μL of BR buffer (40 mM) with different pH and diluted to 2 mL with ultrapure water. Twenty microliters of heparin solution (100 μg mL^{-1}) was added, and the absorption spectra were recorded after a 20-min incubation.

Serum Samples. The serum samples were collected from healthy volunteers and patients in General Hospital of Tianjin Medical University. Each sample was filtered through a 0.45-μm membrane and centrifuged at 10 000 rpm for 10 min to remove particulate matter, and the supernatants were diluted with 10 mM PBS by 5-fold for subsequent analysis.

Procedures for the Detection of Heparin. To detect heparin, 300 μL of cyst-AuNPs solution (2 nM), 1200 μL of ultrapure water, and 500 μL of BR buffer (40 mM, pH 5.0) were sequentially added to the test tube. Twenty microliters of heparin standard solution with various concentrations of sample solution was then added, and the mixture was incubated for 20 min. After 50 μL of try-AuNCs solution (20 mM) was added to the mixture and incubated for 20 s, the fluorescence emission spectra of try-AuNCs were recorded for quantification.

Cytotoxicity of Try-AuNCs. Human cervical carcinoma cell lines (Hela, FR positive), human hepatocarcinoma cell lines (HepG2, FR negative), and mouse embryo fibroblast cell lines (Balb/3T3, control) obtained from China Center for Type Culture Collection (CCTCC) (Wuhan, China) were cultured in Dulbecco's modified Eagle's high glucose medium (DMEM) supplemented with 10% fetal bovine serum (FBS). To evaluate the cytotoxicity of try-AuNCs fluorescent probe, the cell counting assay was conducted by following standard protocols. Cells were plated at a density of 1×10^4 cells per well in 24-well plates in 1000 μL of complete DMEM with 10% FBS and grown for 24 h at 37 °C in 5% CO_2. The try-AuNCs solutions with a wide concentration range from 40 to 4000 μM were subsequently added into the cell and incubated for another 24 h under the same conditions as above. The cells were then washed with 10 mM PBS (pH 7.4), trypsinized with 200 μL of trypsin/EDTA solution, and resuspended to a final volume of 1 mL cell medium for further measurement of cell viability by a cell counting chamber.

Animal Model and in Vivo Tumor Imaging. Nude mice harboring Hela tumors (8 mm) were obtained from the Institute of Hematology & Hospital of Blood Diseases, Chinese Academy of Medical Sciences & Peking Union Medical College (License Number: SCXK-2004-001, Tianjin, China). All animal studies were conducted according to protocols approved by the Animal Ethics Committee of the Institute of Hematology & Hospital of Blood Diseases, Chinese Academy of Medical Sciences & Peking Union Medical College. For in vivo imaging,

the FA-try-AuNCs (200 μM, 200 μL) was intratumorally injected, while the FA-try-AuNCs fluorescent probe (200 μM, 200 μL) was subcutaneously injected into the same site of normal nude mice as a negative control. The mice were anesthetized with intraperitoneal administration of 4% chloral hydrate at a dosage of 400 mg/kg. At the special time points after injection, the fluorescence profiles in normal and Hela tumor-bearing mice were imaged. The resulting images were processed by subtracting the background tissue autofluorescence from the fluorescence from the FA-try-AuNCs probe with the software of the imaging system.

RESULTS AND DISCUSSION

Preparation and Characterization of Try-AuNCs and Cyst-AuNPs. In the present work, try-AuNCs and cyst-AuNPs were integrated to fabricate a selective and sensitive biosensor for heparin based on a novel energy transfer mode, SPEET.[37] Try-AuNCs were synthesized according to the one-pot green and protein-reduction method. Trypsin, containing rich amino acid residues with 7 cysteines and 10 tyrosines that can stabilize the AuNCs, is a strong candidate for the synthesis of protein-stabilized AuNCs. The protective coat of trypsin on the AuNCs ensures the biocompatibility and low-toxicity of try-AuNCs and favors the biosensing and bioimaging application. Moreover, the large overlap of the try-AuNCs excitation spectrum and the cyst-AuNPs SPR absorption spectrum was indispensable for SPEET. In addition, by varying the amount of trypsin and the reaction time, the emission wavelength of the prepared try-AuNCs was adjusted to 690 nm in the near-infrared region (Figures S1 and S2 in the Supporting Information) that is suitable for in vivo bioimaging. As shown in Figure 1A, the prepared try-AuNCs exhibited a bright red fluorescence under UV-irradiation, with the maximal excitation at 520 nm and the maximal emission at 690 nm. Cyst-AuNPs were prepared by the $NaBH_4$-reduction method, and the maximum absorption of the obtained cyst-AuNPs was at 524 nm. Thus, there is a large overlap between the absorption spectrum of AuNPs and the excitation spectrum of AuNCs, meeting the requirement of SPEET (Figure 1A).

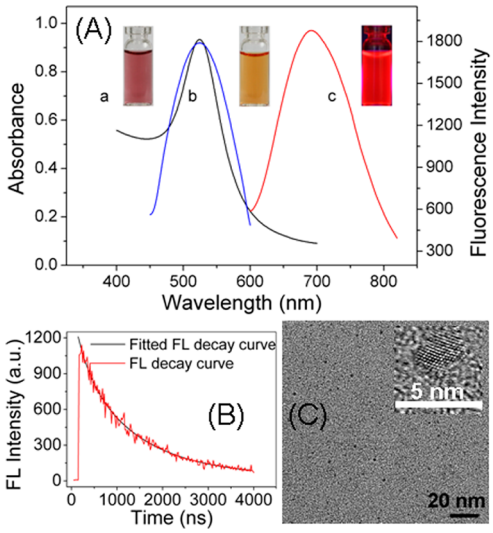

Figure 1. (A) UV absorption spectra (black line) of cyst-AuNPs and photoexcitation (blue line) and photoemission (red line) spectra of the aqueous solution of try-AuNCs. The inset shows the photographs of cyst-AuNPs (a), try-AuNCs under visible (b), and UV (c) light. (B) The fluorescence decay spectra of try-AuNCs. (C) The HRTEM images of try-AuNCs.

The fluorescence lifetime of try-AuNCs was measured to be 1036 ± 20 ns (Figure 1B; Table S1 in the Supporting Information), and the quantum yield was determined to be 6.5%, which are both comparable with those of other protein stabilized gold nanoclusters.[25,51] HRTEM measurement was performed on the prepared nanoclusters and nanoparticles, and at least 150 particles were selected at random to characterize the size distribution of try-AuNCs (Figure 1C; Figures S3 and S4 in the Supporting Information). The prepared try-AuNCs possessed a spherical shape and good size uniformity with a diameter of 2.7 ± 0.4 nm (mainly for the AuNCs core), and the relatively small size was favorable to utilize the try-AuNCs as the in vivo bioimaging probe for tumors.

The XPS spectra (Figure S5a in the Supporting Information) show two distinct doublets, one with the Au $4f_{7/2}$ peak at 83.8 eV and the other at 84.9 eV, assigned to Au(0) (91%) and Au(I) (9%), respectively, confirming the existence of a small amount of Au(I) on the surface to help the stabilization of the AuNCs. Moreover, the S $2p_{3/2}$ peak (Figure S5b in Supporting Information) at 161.9 eV was attributed to a gold thiolate, confirming the covalent interaction of gold nanoclusters with the sulfur groups of the cysteine.[51] The Raman spectra reveal that the trypsin S−S stretching frequency of about 511 cm^{-1} was weakened after the encapsulation of AuNCs (Figure S6 in the Supporting Information), further proving the presence of Au−S bond in the try-AuNCs.[25] FT-IR spectra measurement of trypsin and try-AuNCs (Figure S7 in the Supporting Information) shows a shift of the peak corresponding to the amide I at high wavenumbers from 1639 to 1650 cm^{-1} as expected.[53] It is related to a modification of the secondary structure of the protein backbone predominantly due to the interaction of trypsin and Au. Moreover, the CD spectra of the pure trypsin and try-AuNCs at pH 12 both show a large negative band at around 200 nm from the random coil structure (Figure S8 in Supporting Information), indicating a large conformational change for the try-AuNCs as well as pure trypsin at pH 12, which is in compliance with the previous report.[54] MALDI-TOF-MS analysis shows the molecular weight of the as-prepared try-AuNCs was ∼5 kDa larger than that of trypsin, corresponding to the 25 gold atoms in the AuNCs (Figure S9 in the Supporting Information).[51] Owing to the dependence of emission energy on the number of atoms of fluorescent gold nanoclusters, the prepared try-AuNCs have NIR fluorescent emission at 690 nm.[55]

To employ the try-AuNCs as the bioimaging probe for cancer imaging, we first investigated the potential ability of try-AuNCs to exhibit stable near-infrared fluorescence in the biological media. As shown in Figure S10 (Supporting Information), the common inorganic ions, except Cu^{2+}, Ag^{+}, and Hg^{2+}, did not influence the fluorescence intensity of try-AuNCs at the concentration level of 1 mM or 100 μM. Cu^{2+}, Ag^{+} (100 μM), and Hg^{2+} (10 μM) obviously quenched the fluorescence of try-AuNCs; fortunately, these metal ions are scarce in the biological media. Moreover, the fluorescence of try-AuNCs changed little in the presence of amino acids, proteins, and other biomolecules. In the stability test, try-AuNCs exhibited better stability than GSH-CdTe QDs and comparable stability with other nanoclusters (DNA-AgNCs and lys-AuNCs). We attributed such remarkable photostability to the protection of the trypsin shell and the unique fluorescence properties of AuNCs.

dx.doi.org/10.1021/ac303603f | Anal. Chem. 2013, 85, 3238−3245

Principle of the SPEET/Try-AuNCs Biosensor for Heparin. The SPR property of gold nanoparticles with enhanced local electrical field can increase the absorption cross section and radiative recombination rate of fluorophores and, thus, can be applied for strengthening the donor−acceptor interaction and enhancing the efficiency of surface energy transfer between gold nanoparticles and fluorophores.[37] Figure 2 shows the schematic illustration for selective detection of heparin based on surface plasmon enhanced energy transfer between cyst-AuNPs and try-AuNCs. In the present work, the SPEET between cyst-AuNPs and try-AuNCs was utilized for biosensing. There are two reasons for the formation of SPEET. First, the try-AuNCs were negatively charged (ζ = −9.07 mV) while the cyst-AuNPs were positively charged (ζ = +14.2 mV) in the BR buffer (10 mM, pH 5.0); thus, possible electrostatic interaction made the two close to each other and ensured the surface energy transfer. The large overlap of cyst-AuNPs SPR absorption spectrum with the try-AuNCs excitation spectrum was another indispensable factor for SPEET (Figure 1A). As shown in Figure S11 (Supporting Information), the fluorescence of try-AuNCs was efficiently quenched by cyst-AuNPs. Heparin, a highly negatively charged biopolymer (ζ = −24.3 mV), induced the aggregation of cyst-AuNPs and led to the red-shift of the SPR absorption peak (Figure S12 in the Supporting Information). Moreover, the stronger electrostatic interaction between heparin and cyst-AuNPs increased the distance between cyst-AuNPs and try-AuNCs. Thus, the SPEET was weakened and the fluorescence of try-AuNCs was less quenched.

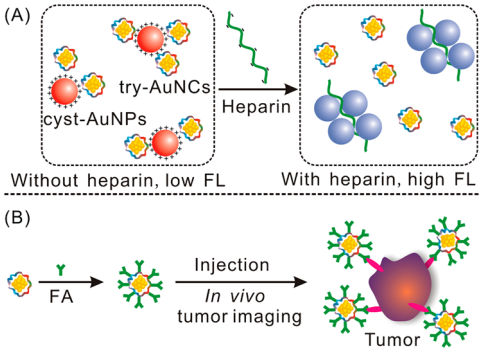

Figure 2. (A) Schematic illustration for selective detection of heparin based on surface plasmon enhanced energy transfer between cyst-AuNPs and try-AuNCs. (B) Schematic illustration for the application of folic acid modified try-AuNCs for in vivo cancer imaging.

According to Chen et al.,[38] the quenching efficiency of the surface energy transfer can be expressed as

$$\chi = \frac{1}{1 + \left(\frac{d}{d_0}\right)^4} \qquad d \propto C^{-3} \tag{1}$$

where χ, d, d_0, and C are the quenching efficiency, the separation distance between cyst-AuNPs and try-AuNCs, the characteristic distance when the surface energy transfer efficiency is reduced to 50%, and the concentration of cyst-AuNPs, respectively. To prove the SPEET responsible for the observed significant fluorescence quenching effect of cyst-AuNPs on try-AuNCs, we plotted the fluorescence quenching efficiency against the cyst-AuNPs concentration according to eq 1. As shown in Figure S11 (Supporting Information), the experimental data can be described quite well by eq 1. Thus, we can conclude that the significant emission quenching in the composite consisting of try-AuNCs and cyst-AuNPs resulted from the surface energy transfer assisted by surface plasmon resonance. To further verify that the try-AuNCs and cyst-AuNPs stayed closed to ensure SPEET because of electrostatic interaction, cyst-AuNPs were replaced by negatively charged AuNPs (citrate-AuNPs) to quench the fluorescence of try-AuNCs. As shown in Figure S13 (Supporting Information), citrate-AuNPs with SPR absorption peak at 520 nm also quenched the fluorescence of try-AuNCs, and the quenching behavior followed eq 1. However, the quenching efficiency of citrate-AuNPs was much lower than cyst-AuNPs at the same concentration level, indicating that the distance between citrate-AuNPs and try-AuNCs was longer than that between cyst-AuNPs and try-AuNCs due to the weaker electrostatic interaction.

Factors Affecting the Detection of Heparin by the Proposed SPEET/try-AuNCs Biosensors. To achieve optimal detection performance, we carefully optimized the assay conditions, including the time for the reaction between heparin and cyst-AuNPs and for the reaction between try-AuNCs and heparin-cyst-AuNPs and the pH value of 10 mM BR buffer used in the assay.

The effect of time for the reaction of heparin with cyst-AuNPs was investigated in BR buffer (10 mM, pH 5.0) with the heparin concentration of 0.50, 0.75, and 1.00 μg mL^{-1}. Heparin induced a red-shift of the absorption peak of cyst-AuNPs from 520 to 650 nm (Figure S12 in the Supporting Information). The ratio of $A_{650\ nm}/A_{520\ nm}$ is usually used to quantify the interaction of heparin with cyst-AuNPs.[48] As shown in Figure 3A, the ratio of $A_{650\ nm}/A_{520\ nm}$ increased to the maximum within 15 min and remained stable with further increase of the reaction time, indicating the reaction between heparin and cyst-AuNPs was finished in 15 min. For further experiments, a reaction time of 20 min was used to ensure complete reaction.

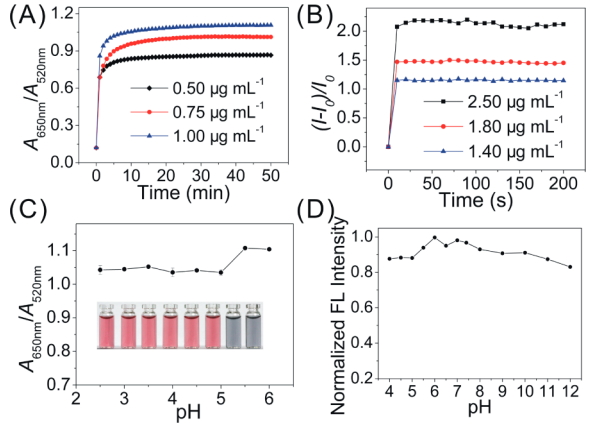

Figure 3. Optimization of the proposed SPEET/try-AuNCs biosensor for heparin: (A) Effect of time on the reaction between heparin (0.50, 0.75, 1.00 μg mL^{-1}) and cyst-AuNPs; (B) effect of time on the reaction between heparin (1.40, 1.80, 2.50 μg mL^{-1})-cyst-AuNPs and try-AuNCs; (C) effect of the pH value of BR buffer (10 mM) on the interaction between heparin and cyst-AuNPs. The inset photographs show the pH stability of cyst-AuNPs in BR buffer (10 mM). (D) The pH stability of try-AuNCs.

To pursue the optimal incubation time for try-AuNCs with heparin-cyst-AuNPs, the effect of time for the reaction of try-

dx.doi.org/10.1021/ac303603f | Anal. Chem. 2013, 85, 3238−3245

AuNCs with heparin-cyst-AuNPs was investigated in BR buffer (10 mM, pH 5.0) with heparin concentration of 1.40, 1.80, and 2.50 μg mL^{-1}. The response $((I - I_0)/I_0$, where I_0 and I represent the fluorescence of the mixture of try-AuNCs and cyst-AuNPs in the absence of heparin and in the presence of heparin, respectively) increased to the maximum within 10 s and remained stable with further increase of the reaction time, indicating the reaction between try-AuNCs and heparin-cyst-AuNPs was very rapid (Figure 3B). For further experiments, a reaction time of 20 s was used to ensure complete reaction.

The effect of pH on the interaction between heparin and cyst-AuNPs in a pH range of 2.5−6.0 in 10 mM BR buffer was tested as a primary step to obtain optimum pH value of BR buffer for incubation in the SPEET/try-AuNCs biosensor. Although a better response ($A_{650\ nm}/A_{520\ nm}$) of cyst-AuNPs to heparin was achieved at the pH range of 5.5 to 6.0, the cyst-AuNPs tended to be aggregated in pH >5.0 (Figure 3C). Considering that the fluorescence of try-AuNCs remained stable in acidic-to-basic environments spanning pH 4−12 (Figure 3D), we chose 10 mM BR buffer (pH 5.0) as the reaction media for the bioassay.

Specificity. To test the specificity of the developed SPEET/try-AuNCs biosensor for heparin, twenty amino acids, fourteen common biomolecules, and fourteen common inorganic ions were chosen for the interference study under the same assay conditions for heparin determination. The SPEET biosensor response arises from the aggregation of cyst-AuNPs induced by electrostatic attraction between the positively charged cyst-AuNPs and highly negatively charged polyanionic heparin, and the increase of the distance between cyst-AuNPs and try-AuNCs in the presence of large size of molecules. Thus, the small or amphoteric biomolecules, such as amino acids, GSH, lactic acid, and glucose, produced little response in the SPEET assay at 100 μM level. Serum proteins, such as HSA (p*I* 4.6−5.3, ζ = −3.08 mV), IgG (p*I* 8.6, ζ = +9.41 mV), insulin (p*I* 5.3, ζ = +1.23 mV), lysozyme (p*I* 10.7, ζ = +8.40 mV), cyt-C (p*I* 10.7, ζ = +6.46 mV), transferrin (p*I* 4.7−5.2, ζ = −1.43 mV), fibrinogen (p*I* 5.1−6.3, ζ = +2.71 mV), hemoglobin (p*I* 7.1, ζ = +2.70 mV), myoglobin (p*I* 6.8, ζ = +2.63 mV), and zonolysin (p*I* 8.1−8.6, ζ = +3.77 mV),[56] had positive charge or weak negative charge in the reaction media of BR buffer (10 mM, pH 5.0) and hardly induced cyst-AuNPs aggregation through an electrostatic mechanism, thus producing negligible response to the developed SPEET/try-AuNCs biosensor compared with 2.5 μg mL^{-1} heparin (Figure 4). In addition, the common inorganic ions at the concentration of the physiological level produced negligible interference for the proposed heparin biosensor. All the above data indicate excellent selectivity of our proposed SPEET/try-AuNCs biosensor toward heparin.

Analytical Performance of the SPEET/Try-AuNCs Biosensor. The figures of merit for the developed SPEET/try-AuNCs biosensor for heparin are summarized in Table 1. The proposed method gave a linear range of 0.1−4.0 μg mL^{-1} (Figure 5) and a detection limit (3*s*) of 0.05 μg mL^{-1} for the detection of heparin. The precision (relative standard deviation, RSD) for eleven replicate detections of 2.50 μg mL^{-1} heparin was 1.1%. Compared with previous optical methods for heparin, the proposed SPEET/try-AuNCs biosensor gave comparable[48,57,58] or better[39,40,43,59,60] detection limit (Table S2 in the Supporting Information). The developed SPEET/try-AuNCs biosensor was applied to the determination of heparin in human serum samples to demonstrate its applicability for real sample analysis. The recoveries of the spiked serum samples ranged from 97% to 100%. The analytical results for the hospital serum samples from operation patients determined by the developed method were in good agreement with those determined by the medical diagnostic method in the hospital, indicating our developed SPEET/try-AuNCs biosensor possessed excellent applicability for real sample analysis (Table 2; Table S3 in the Supporting Information).

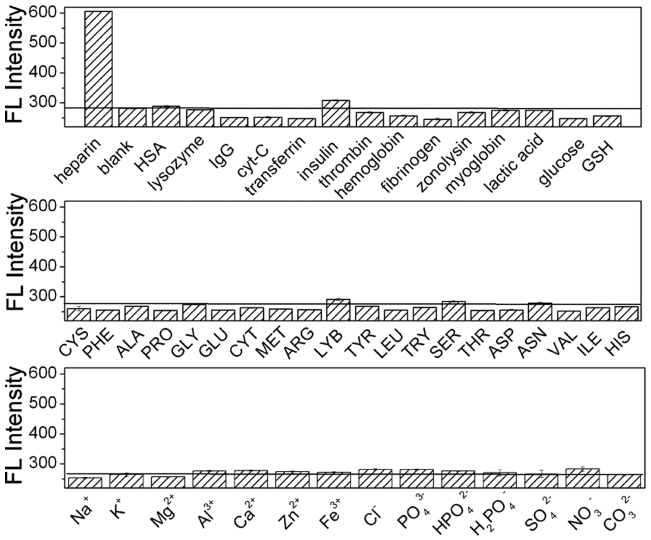

Figure 4. Specificity test of the developed SPEET/try-AuNCs biosensor for heparin (2.5 μg mL^{-1}) over other biomolecules and inorganic ions. Concentrations: amino acids, 100 μM; HSA and IgG, 1 mM; insulin, lysozyme, cyt-C, transferrin, fibrinogen, hemoglobin, myoglobin, and zonolysin, 10 μM; glucose, lactic acid, and GSH, 100 μM; thrombin, 1 μM; K^+ and Na^+, 10 mM; Ca^{2+} and Mg^{2+}, 2 mM; Al^{3+}, Zn^{2+}, and Fe^{3+}, 100 μM; Cl^-, NO_3^-, SO_4^{2-}, CO_3^{2-}, PO_4^{3-}, HPO_4^{2-}, and $H_2PO_4^-$, 1 mM.

Table 1. Analytical Figures of Merit of the SPEET/Try-AuNCs Biosensor for Heparin

detection limit (3*s*)/μg mL^{-1}	0.05
linear range/μg mL^{-1}	0.1−4.0
calibration function (R, $(I - I_0)/I_0$; C, conc./μg mL^{-1})	R = 0.80C + 0.03
correlation coefficient (γ^2)	0.9981
precision (RSD, n = 11)/%	1.1 (2.50 μg mL^{-1})

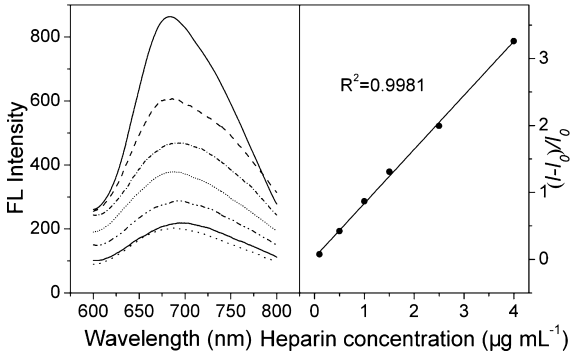

Figure 5. Fluorescence emission spectra of the SPEET try-AuNCs biosensor in the presence of heparin at various concentrations and the corresponding calibration curve. All solutions were prepared in 10 mM BR buffer (pH 5.0).

FA Functionalized Try-AuNCs for in Vivo Tumor Bioimaging. The folic acid modification of try-AuNCs was

dx.doi.org/10.1021/ac303603f | *Anal. Chem.* 2013, 85, 3238−3245

Table 2. Analytical Results for the Determination of Heparin in Human Serum Samples Using the Proposed SPEET/Try-AuNCs Biosensor

sample	concentration of spiked heparin in final solution for analysis/μg mL^{-1}	concentration found (mean ± s, n = 3)/μg mL^{-1}	recovery (mean ± s, n = 3) /%
serum-1	0.50	0.50 ± 0.03	100 ± 6
	2.00	1.98 ± 0.02	99 ± 1
serum-2	0.50	0.48 ± 0.02	97 ± 5
	2.00	1.96 ± 0.03	98 ± 2
serum-3	0.50	0.50 ± 0.01	99 ± 2
	2.00	1.96 ± 0.04	98 ± 2

realized by the EDC activation method, and the bioconjugation result was characterized by FT-IR (Figure S7 in the Supporting Information). All the characteristic vibrational modes associated with FA, such as C−H stretching at 2943 cm^{-1} and aromatic ring stretch of the pyridine and p-amino benzoic acid moieties in the range of 1476−1695 cm^{-1}, were clearly seen in the FT-IR spectra of FA and FA-try-AuNCs, and the line broadening appearing over 1652−1350 cm^{-1} is indicative of the covalent linkage of FA with try-AuNCs.[52]

Effective biomaterials for use as contrast agents should be safe and nontoxic to cells and tissues. Thereby, the toxicity study is crucial for the potential applications of try-AuNCs fluorescent probe. In the present work, the toxicity of the try-AuNCs was evaluated by in vitro investigations of different cell lines (3T3, Hela, HepG-2) with cell counting assay. The results indicate no obvious toxicity of try-AuNCs on normal cell line (3T3) and FR positive (Hela) and negative (HepG-2) tumor cell lines (Figure S14 in the Supporting Information). The component design of try-AuNCs probe favors the observed low toxicity of the nanoclusters. Trypsin is a biological enzyme produced by the cell, which exists widely in biological media and plays a key role in life metabolism processes. The protective coat of trypsin on the probe could play a significant role in maintaining the biofriendly nature of the nanoprobe. Further modification of try-AuNCs with FA did not increase the cytotoxicity of the NIR probe, as the FA moiety is vitamin B11, a naturally occurring product that plays an important role in DNA synthesis. The cytotoxicity study shows that the NIR fluorescent probe has no obvious toxicity on different cell lines over a wide concentration range between 40 and 4000 μM.

To demonstrate the feasibility of the prepared FA-try-AuNCs fluorescent probe for in vivo tumor imaging, the FA-try-AuNCs were intratumorally injected into the tumor-bearing mice, followed by real-time monitoring and imaging. As shown in Figure 6, upon injection of the probe into the tumor-bearing mice, the fluorescence signal focusing on the tumor was immediately detected due to the FR on the tumor cell surface, and the NIR fluorescence signal in tumors was detectable for up to 12 h. Furthermore, FA-try-AuNCs with the same amount were subcutaneously injected into the same site of normal nude mice as a control, and the fluorescence signal was detected all over the whole body of mice within 5 min and gradually disappeared after 12 h, indicating the FA-try-AuNCs can spread and be metabolized by the mice. We also observed that the clearance rate of FA-try-AuNCs probe in the tumor site was much slower than in normal tissues, probably because the high affinity of the FA to target cancer cells prevented the probes from degradation and metabolism. An additional control experiment was conducted by subcutaneous injection of FA-try-AuNCs into the tumor-bearing mice. Similar to the normal control mice, FA-try-AuNCs were initially distributed all over

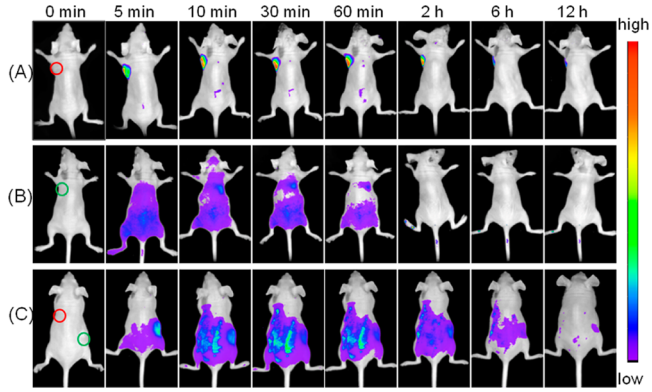

Figure 6. In vivo time-dependence tumor imaging of the Hela tumor-bearing nude mice and normal nude mice by the NIR fluorescence imaging system. The FA-try-AuNCs fluorescent probe was intratumorally injected into the tumor-bearing mice (A) and subcutaneously injected into the left forelimb region of the normal nude mice (B) and tumor-bearing mice (C). The red cycle and green cycle indicate the tumor site and injection site, respectively.

the body. However, the probe was increasingly accumulated in the tumor site as time extended and was gradually metabolized slower than in normal tissues. The above results demonstrate that the FA-try-AuNCs probe can target and image the tumor with high specificity and good biocompatibility and positively support the FA-try-AuNCs as a promising specific fluorescent probe for in vivo cancer imaging.

CONCLUSIONS

In summary, we have reported the preparation and application of the near-infrared fluorescent trypsin stabilized gold nanoclusters for biosensing and bioimaging application. The novel energy transfer mode, SPEET, was first utilized for fabricating a biosensor for heparin. In vivo study of the dynamic behavior and targeting ability of try-AuNCs probe with folic acid modification to Hela tumor bearing mice and normal nude mice validated the high specific affinity of FA-try-AuNCs probe to FR positive tumors. All the results show that the prepared try-AuNCs have great potential as multifunctional biomaterials for biosensing biomolecules with SPEET mode and in vivo cancer imaging with high targeting ability.

ASSOCIATED CONTENT

Supporting Information

Additional information as noted in the text. This material is available free of charge via the Internet at http://pubs.acs.org.

AUTHOR INFORMATION

Corresponding Author

*Fax: (86)22-23506075. E-mail: xpyan@nankai.edu.cn.

Notes

The authors declare no competing financial interest.

■ ACKNOWLEDGMENTS

This work was supported by the National Basic Research Program of China (Grant 2011CB707703), the National Natural Science Foundation of China (Grants 21275079, 20935001), the Fundamental Research Funds for the Central Universities, and the Tianjin Natural Science Foundation (Grant 10JCZDJC16300).

■ REFERENCES

(1) Weissleder, R. *Science* **2006**, *312*, 1168−1171.
(2) Weissleder, R.; Pittet, M. J. *Nature* **2008**, *452*, 580−589.
(3) Jennings, L. E.; Long, N. J. *Chem. Commun.* **2009**, 3511−3524.
(4) Larson, D. R.; Zipfel, W. R.; Williams, R. M.; Clark, S. W.; Bruchez, M. P.; Wise, F. W.; Webb, W. W. *Science* **2003**, *300*, 1434−1436.
(5) Pinaud, F.; Michalet, X.; Bentolila, L. A.; Tsay, J. M.; Doose, S.; Li, J. J.; Iyer, G.; Weiss, S. *Biomaterials* **2006**, *27*, 1679−1687.
(6) Bagalkot, V.; Zhang, L.; Levy-Nissenbaum, E.; Jon, S.; Kantoff, P. W.; Langer, R.; Farokhzad, O. C. *Nano Lett.* **2007**, *7*, 3065−3070.
(7) Chatteriee, D. K.; Rufalhah, A. J.; Zhang, Y. *Biomaterials* **2008**, *29*, 937−943.
(8) Kim, J.; Kim, H. S.; Lee, N.; Kim, T.; Kim, H.; Yu, T.; Song, I. C.; Moon, W. K.; Hyeon, T. *Angew. Chem., Int. Ed.* **2008**, *47*, 8438−8441.
(9) Shang, L.; Dong, S.; Nienhaus, G. U. *Nano Today* **2011**, *6*, 401−418.
(10) Diez, I.; Ras, R. H. A. *Nanoscale* **2011**, *3*, 1963−1970.
(11) Wang, H.-H.; Lin, C.-A. J.; Lee, C.-H.; Lin, Y.-C.; Tseng, Y.-M.; Hsieh, C.-L.; Chen, C.-H.; Tsai, C.-H.; Hsieh, C.-T.; Shen, J.-L.; Chan, W.-H.; Chang, W. H.; Yeh, H.-I. *ACS Nano* **2011**, *5*, 4337−4344.
(12) Huang, C. C.; Chiang, C. K.; Lin, Z. H.; Lee, K. H.; Chang, H. T. *Anal. Chem.* **2008**, *80*, 1497−1504.
(13) Huang, C.-C.; Chen, C.-T.; Shiang, Y.-C.; Lin, Z.-H.; Chang, H.-T. *Anal. Chem.* **2009**, *81*, 875−882.
(14) Lin, Y. H.; Tseng, W. L. *Anal. Chem.* **2010**, *82*, 9194−9200.
(15) Liu, Y. L.; Ai, K. L.; Cheng, X. L.; Huo, L. H.; Lu, L. H. *Adv. Funct. Mater.* **2010**, *20*, 951−956.
(16) Li, L. L.; Liu, H. Y.; Shen, Y. Y.; Zhang, J. R.; Zhu, J. J. *Anal. Chem.* **2011**, *83*, 661−665.
(17) Wang, X. X.; Wu, Q.; Shan, Z.; Huang, Q. M. *Biosens. Bioelectron.* **2011**, *26*, 3614−3619.
(18) Wei, H.; Wang, Z. D.; Zhang, J. O.; House, S.; Gao, Y. G.; Yang, L. M.; Robinson, H.; Tan, L. H.; Xing, H.; Hou, C. J.; Robertson, I. M.; Zuo, J. M.; Lu, Y. *Nat. Nanotechnol.* **2011**, *6*, 92−96.
(19) Wen, F.; Dong, Y. H.; Feng, L.; Wang, S.; Zhang, S. C.; Zhang, X. R. *Anal. Chem.* **2011**, *83*, 1193−1196.
(20) Guo, W. W.; Yuan, J. P.; Dong, Q. Z.; Wang, E. K. *J. Am. Chem. Soc.* **2010**, *132*, 932−933.
(21) Yeh, H. C.; Sharma, J.; Han, J. J.; Martinez, J. S.; Werner, J. H. *Nano Lett.* **2010**, *10*, 3106−3110.
(22) Zhou, Z. X.; Du, Y.; Dong, S. J. *Biosens. Bioelectron.* **2011**, *28*, 33−37.
(23) He, H.; Xie, C.; Ren, J. C. *Anal. Chem.* **2008**, *80*, 5951−5957.
(24) Wu, X.; He, X.; Wang, K.; Xie, C.; Zhou, B.; Qing, Z. *Nanoscale* **2010**, *2*, 2244−2249.
(25) Liu, C.-L.; Wu, H.-T.; Hsiao, Y.-H.; Lai, C.-W.; Shih, C.-W.; Peng, Y.-K.; Tang, K.-C.; Chang, H.-W.; Chien, Y.-C.; Hsiao, J.-K.; Cheng, J.-T.; Chou, P.-T. *Angew. Chem., Int. Ed.* **2011**, *50*, 7056−7060.
(26) Polavarapu, L.; Manna, M.; Xu, Q.-H. *Nanoscale* **2011**, *3*, 429−434.
(27) Shang, L.; Azadfar, N.; Stockmar, F.; Send, W.; Trouillet, V.; Bruns, M.; Gerthsen, D.; Nienhaus, G. U. *Small* **2011**, *7*, 2614−2620.
(28) Shang, L.; Dorlich, R. M.; Brandholt, S.; Schneider, R.; Trouillet, V.; Bruns, M.; Gerthsen, D.; Nienhaus, G. U. *Nanoscale* **2011**, *3*, 2009−2014.
(29) Sun, C.; Yang, H.; Yuan, Y.; Tian, X.; Wang, L.; Guo, Y.; Xu, L.; Lei, J.; Gao, N.; Anderson, G. J.; Liang, X.-J.; Chen, C.; Zhao, Y.; Nie, G. *J. Am. Chem. Soc.* **2011**, *133*, 8617−8624.
(30) Chen, H.; Li, S.; Li, B.; Ren, X.; Li, S.; Mahounga, D. M.; Cui, S.; Gu, Y.; Achilefu, S. *Nanoscale* **2012**, *4*, 6050−6064.
(31) Jain, P. K.; Huang, X. H.; El-Sayed, I. H.; El-Sayed, M. A. *Acc. Chem. Res.* **2008**, *41*, 1578−1586.
(32) Liu, J.-M.; Wang, H.-F.; Yan, X.-P. *Analyst* **2011**, *136*, 3904−3910.
(33) Link, S.; EI-Sayed, M. A. *Annu. Rev. Phys. Chem.* **2003**, *54*, 331−366.
(34) Eustis, S.; El-Sayed, M. A. *Chem. Soc. Rev.* **2006**, *35*, 209−217.
(35) Yun, C. S.; Javier, A.; Jennings, T.; Fisher, M.; Hira, S.; Peterson, S.; Hopkins, B.; Reich, N. O.; Strouse, G. F. *J. Am. Chem. Soc.* **2005**, *127*, 3115−3119.
(36) Chen, Y.; O'Donoghue, M. B.; Huang, Y. F.; Kang, H. Z.; Phillips, J. A.; Chen, X. L.; Estevez, M. C.; Yang, C. Y. J.; Tan, W. H. *J. Am. Chem. Soc.* **2010**, *132*, 16559−16570.
(37) Griffin, J.; Singh, A. K.; Senapati, D.; Rhodes, P.; Mitchell, K.; Robinson, B.; Yu, E.; Ray, P. C. *Chem.—Eur. J.* **2009**, *15*, 342−351.
(38) Chen, C.-W.; Wang, C.-H.; Wei, C.-M.; Hsieh, C.-Y.; Chen, Y.-T.; Chen, Y.-F.; Lai, C.-W.; Liu, C.-L.; Hsieh, C.-C.; Chou, P.-T. *J. Phys. Chem. C* **2009**, *114*, 799−802.
(39) Wright, A. T.; Zhong, Z.; Anslyn, E. V. *Angew. Chem., Int. Ed.* **2005**, *44*, 5679−5682.
(40) Wang, M.; Zhang, D.; Zhang, G.; Zhu, D. *Chem. Commun.* **2008**, 4469−4471.
(41) Niidome, T.; Nakashima, K.; Takahashi, H.; Niidome, Y. *Chem. Commun.* **2004**, 1978−1979.
(42) Korir, A. K.; Larive, C. K. *Anal. Bioanal. Chem.* **2009**, *393*, 155−169.
(43) Zhan, R. Y.; Fang, Z.; Liu, B. *Anal. Chem.* **2010**, *82*, 1326−1333.
(44) Yan, H.; Wang, H.-F. *Anal. Chem.* **2011**, *83*, 8589−8595.
(45) Gu, X. G.; Zhang, G. X.; Zhang, D. Q. *Analyst* **2012**, *137*, 365−369.
(46) Dai, Q.; Liu, W. M.; Zhuang, X. Q.; Wu, J. S.; Zhang, H. Y.; Wang, P. F. *Anal. Chem.* **2011**, *83*, 6559−6564.
(47) Fu, X. L.; Chen, L. X.; Li, J. H.; Lin, M.; You, H. Y.; Wang, W. H. *Biosens. Bioelectron.* **2012**, *34*, 227−231.
(48) Cao, R.; Li, B. X. *Chem. Commun.* **2011**, *47*, 2865−2867.
(49) Pu, Q. S.; Elazazy, M. S.; Alvarez, J. C. *Anal. Chem.* **2008**, *80*, 6532−6536.
(50) Gemene, K. L.; Meyerhoff, M. E. *Anal. Chem.* **2010**, *82*, 1612−1615.
(51) Xie, J.; Zheng, Y.; Ying, J. Y. *J. Am. Chem. Soc.* **2009**, *131*, 888−889.
(52) Retnakumari, A.; Setua, S.; Menon, D.; Ravindran, P.; Muhammed, H.; Pradeep, T.; Nair, S.; Koyakutty, M. *Nanotechnology* **2010**, *21*, 055103.
(53) Mizutani, K.; Toyoda, M.; Mikami, B. *Biochim. Biophys. Acta, Gen. Subj.* **2012**, *1820*, 203−211.
(54) Kawasaki, H.; Yoshimura, K.; Hamaguchi, K.; Arakawa, R. *Anal. Sci.* **2011**, *27*, 591−596.
(55) Zheng, J.; Zhang, C. W.; Dickson, R. M. *Phys. Rev. Lett.* **2004**, *93*, 077402.
(56) Lacerda, S. H. D. P.; Park, J. J.; Meuse, C.; Pristinski, D.; Becker, M. L.; Karim, A.; Douglas, J. F. *ACS Nano* **2009**, *4*, 365−379.
(57) Wang, S.; Chang, Y.-T. *Chem. Commun.* **2008**, 1173−1175.
(58) Pu, K.-Y.; Liu, B. *Macromolecules* **2008**, *41*, 6636−6640.
(59) Pu, K.-Y.; Liu, B. *Adv. Funct. Mater.* **2009**, *19*, 277−284.
(60) Sun, W.; Bandmann, H.; Schrader, T. *Chem.—Eur. J.* **2007**, *13*, 7701−7707.